DOI: https://doi.org/10.14311/TPFM.2026.010

METHODOLOGY FOR VELOCITY FIELD MEASUREMENTS IN PILOT-SCALE STIRRED VESSELS USING 2-D PARTICLE TRACKING VELOCIMETRY

O. Gebouský [1, 2], V. Bílek [1, 2], J. Haidl [1]

[1] **Czech Academy of Sciences, Institute of Hydrology, Pod Paťankou 30/5, Prague 160 00, Czech Republic**

[2] **Department of Chemical Engineering, Faculty of Chemical Engineering, University of Chemistry and Technology, Technická 5, Prague 166 28, Czech Republic**

Abstract

Reliable validation of computational fluid dynamics (CFD) simulations of mixing in pilot- and industrial-scale vessels is hindered by the scarcity of experimental data, particularly for non-standard geometries and operating conditions. To address this gap, a large-scale Particle Tracking Velocimetry (PTV) measurement methodology was developed, implemented, and critically evaluated. The methodology was applied to a pilot-scale rectangular stirred vessel operated in four configurations, comprising single- and dual-impeller arrangements with either Rushton turbines or pitched blade turbines. The contribution presents a comprehensive description of the experimental setup, including illumination, image acquisition, and seeding strategy, as well as the data processing workflow. Particular attention is given to trajectory reconstruction, validation criteria, and filtering procedures used to remove spurious or physically inconsistent particle trajectories. The resulting velocity and turbulent kinetic energy fields are analyzed with emphasis on their applicability for the validation of Reynolds-Averaged Navier–Stokes simulations. The advantages and limitations of the proposed PTV approach are critically discussed. While the methodology enables spatially resolved velocity measurements over large volumes and captures key flow structures, several shortcomings are identified. These include reduced accuracy of velocity estimates in high-speed regions near impeller discharge, limited reliability of turbulent kinetic energy estimation, and particle settling effects in low-velocity zones. Overall, the study provides practical guidance on the capabilities and limitations of large-scale PTV measurements and offers valuable experimental insights for validating CFD models of mixing in complex, industrially relevant vessels.

Keywords: particle tracking velocimetry, PTV, CFD validation, stirred vessel.

1 Introduction

Computational Fluid Dynamics (CFD) offers tools to simulate flows in almost all environments and produce potentially valuable analyses of these flows. The critical issue with many simulations is the reliability of the calculated data due to a lack of validation of the CFD techniques against experimental data under the respective operating conditions. In the absence of systematic validation, engineers are compelled to base their decisions on unverified data; that approach is more aligned with a heuristic trial-and-error methodology than with a rigorous, scientifically grounded one.

Simulations of the hydrodynamics of mechanically mixed vessels are a specific case of flow simulation, given the presence of rotating components, flow recirculation, and separated flows. The scientific literature provides numerous numerical and experimental results proving that the CFD methods are capable of providing sufficiently accurate hydrodynamics predictions. However, the only configuration that has been deeply studied is the *Standard Tank Configuration* (STC), a cylindrical tank equipped with four wall baffles and a centrally positioned impeller. This mixed vessel configuration is the most commonly used in the industry. Consequently, the experimental data for the STC are available in the largest quantity and detail. However, for other industrially relevant configurations, experimental data are not yet available. An example of such a configuration is a flocculation tank used at water treatment facilities - large rectangular tank equipped with one or multiple impellers. That tanks are typically installed at water treatment facilities as flocculation tanks. Reliable flow simulations of such vessels would enable optimization of their hydrodynamics, which is critical because it directly affects the water treatment performance.

To obtain quantitative experimental data, contemporary scientific research employs a variety of advanced diagnostic techniques; most relevant for our purpose are Doppler shift-based methods such as Laser Doppler Velocimetry (LDV) and Planar Doppler Velocimetry (PDV), and image-based methods such as Particle Image Velocimetry (PIV) and Particle Tracking Velocimetry (PTV). Our aim is to validate a flow simulation methodology that is suitable for industrial applications, flocculation tanks in particular. Reliable validation requires spatially resolved hydrodynamic data across the entire apparatus volume. Therefore, the application of LDV was deemed impractical, as it is a single-point, single-component technique that requires traversing the probe across a dense grid from multiple directions to scan the required area for multiple velocity components. These drawbacks can be partially mitigated by PDV, which can measure large surface areas (up to 1 m^2) at once. However, it relies on Doppler shifts associated with high-speed (primarily aerodynamic) flows ($> 100\,\mathrm{m/s}$); in the low-speed regime characteristic for stirred tanks ($< 5\,\mathrm{m/s}$), the Doppler shift is negligible, rendering this method unusable for tank flow characterization [1].

Both image-based methods rely on analyzing the motion of seeding particles in fluid; however, they differ in the employed data evaluation methodologies. The PIV technique is a statistical method that determines the most probable displacement of an ensemble of tracer particles within interrogation windows, thereby yielding the local displacement vectors within each window. The method requires a relatively high concentration of seeding particles, which, in turn, imposes stringent requirements on both the illumination and the optical system. This constraint renders measurements over extended regions or within the bulk of comparatively large vessels technically challenging or even unfeasible. Consequently, the measurement domain is typically limited to a relatively small area of approximately 400 cm^2; hence, it is usually used for vessels with a maximum volume of several tens of liters. In contrast, the PTV tracks individual particles over time and provides their trajectories, which consequently enables the calculation of velocity. Compared with PIV, PTV operates effectively with substantially lower concentrations of seeding particles; therefore, the illuminating light sheet can propagate over greater distances. These characteristics enhance the feasibility of accurately measuring flow velocities within the bulk region of a liquid in pilot-scale vessels.

Based on prior comparisons of common experimental techniques, we selected the PTV technique as the most suitable for the intended purpose. In this contribution, we present our large-scale 2-D PTV methodology for measuring the flow field within a pilot-scale vessel, detailing the experimental setup, image acquisition, data evaluation algorithm, and the strengths and limitations of the approach.

2 Experimental setup

Stirred tank Particle tracking velocimetry (PTV) experiments were conducted in a rectangular stirred vessel with a volume of ≈ 195 L, using tap water as the operating fluid ($T \approx 20\,°\mathrm{C}$). The vessel's front and side walls are made of glass, and the tank is equipped with a floating lid to suppress gas entrainment and unwanted reflections from the free surface. The vessel was operated in a single- or double-stirrer configuration, using either a 6-bladed Rushton turbine (RT) or a 4-bladed pitched-blade turbine (PBT) with a diameter D of 130 mm (see Fig. 1). The stirrers were mounted with clearance C of 133 mm ($C/H = 1/3$). While the PBT configurations operated as down-pumping (rotating clockwise from a top view), in the two-RTs configuration, the stirrers rotated in counter-rotation (left RT clockwise, central RT counter-clockwise). The used stirrer rotational speeds are summarized in Tab. 2 a) and are based on mean velocity gradients $\overline{G}$ of 40 s^{-1} and 100 s^{-1} (assumed power numbers: $N_{\mathrm{p,\,RT}} = 5$, $N_{\mathrm{p,\,PBT}} = 1$), which are commonly used for a flocculation at water treatment facilities.

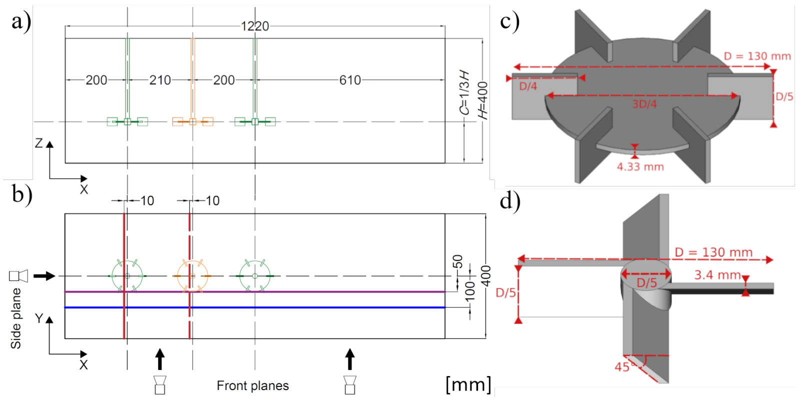

Figure 1: Experimental pilot-scale stirred vessel in the single- and double-stirrer configuration (orange and green stirrers) from (a) front and (b) top views with depicted measurement front and side planes (purple, blue, red). Scheme of the (c) Rushton turbine and (d) pitched blade turbine with marked dimensions used in this work (taken from [2]).

Image acquisition A total of three vertical planes were measured in the experimental apparatus - two front planes of the vessel (X-Z planes 5 cm and 10 cm in front of the stirrer/stirrers) and one side plane of the apparatus (Y-Z plane 1 cm in front of the left stirrer), see Fig. 1b). The flow fields in the X-Z planes were measured separately for the left and right halves of the tank, thereby achieving a higher resolution (pixel size of $L_{px} \approx 0.6\,\mathrm{mm/px}$) and better illumination of the measured plane. The illumination system consists of four line laser modules (520 nm wavelength) with a combined power of 4×135 mW; for the measurements in *X-Z* plane, another module with a power of 8×30 mW was used for additional illumination from the opposite side of the vessel. The thickness of the plane was ≈ 8 mm. A high-speed Dantec Dynamics SpeedSense VEO CCD camera with Laowa 60 mm 2:1 macro lens and 1280×800 px resolution was used for shooting. The objective of the measurement was to obtain the time-averaged velocity field in the measured planes for the validation of RANS simulations of this stirred vessel. Therefore, a relatively long 50 s time period at a sampling frequency of $f = 1000\,\mathrm{Hz}$ was used, ensuring sufficient time to detect even low-frequency speed fluctuations and to identify enough trajectories in the whole measurement plane.

Seeding particles The acrylonitrile-butadiene-styrene (ABS, density $\rho_P \approx 1040\,\mathrm{kg/m^3}$) microbeads were used as seeding particles for PTV experiments. The particles were prepared using a 3D printer with ABS filament, on which cylinders 4 cm in diameter were printed (50% infill, grid pattern). The cylinder was mounted in a lathe, and the particles were rasped off. The resulting particles were sieved, and a fraction d_p of 200−300 µm was used for subsequent measurements in mass concentration of $25\,\mathrm{g/m^3}$. Particles larger than 300 µm (which did not pass through the upper sieve) were chopped with a knife blender and sieved again. To suppress particle aggregation, $50\,\mathrm{g/m^3}$ of sodium dodecyl sulfate was also dissolved in the batch. The particles were slightly negatively buoyant, with an experimentally measured settling velocity of (2.0 ± 0.3) mm/s, which was accounted for in the subsequent processing of the results.

3 Data evaluation

Particles tracking First, the raw images from the high-speed camera were masked to eliminate the influence of illuminated edges, impellers, and other noisy parts of the image. Next, the photos were binary thresholded (default: 50/255) to clearly distinguish the particles from the background. The images prepared in this way were subsequently processed with a modified version of the TracTrac software [3], which filters out static (false) signals and tracks the positions of the illuminated particles if they appear in at least three consecutive frames. The labeled particles and their positions in individual images then served as input data for perspective correction and trajectory evaluation.

Perspective and scale correction A plane-to-plane homography was used to correct and scale the original extracted particle positions [4]. Before each experiment, a calibration images of one ($Y - Z$ plane) or two ($X - Z$ planes) calibration planes were taken, each with $N = 4$ marked calibration points of known real-world coordinates (X, Y, Z), and the image coordinates (x, z) of these points were identified. To estimate the homography vector $\boldsymbol{h}$, the direct linear transform (DLT) method was used, consisting of solving a system of $2N$ linear equations for points $i = 1 \longrightarrow N$ as follows, on the example of the *X-Z* plane:

$$\begin{pmatrix} x_1 & z_1 & 1 & 0 & 0 & 0 & -x_1X_1 & -z_1X_1 \\ \vdots & \vdots & \vdots & \vdots & \vdots & \vdots & \vdots & \vdots \\ x_N & z_N & 1 & 0 & 0 & 0 & -x_NX_N & -z_NX_N \\ 0 & 0 & 0 & x_1 & z_1 & 1 & -x_1Z_1 & -z_1Z_1 \\ \vdots & \vdots & \vdots & \vdots & \vdots & \vdots & \vdots & \vdots \\ 0 & 0 & 0 & x_N & z_N & 1 & -x_NZ_N & -z_NZ_N \end{pmatrix} \boldsymbol{h} = \begin{pmatrix} X_i \\ \vdots \\ X_N \\ Z_i \\ \vdots \\ Z_N \end{pmatrix}. \tag{1}$$

In the cases of $Y - Z$ plane measurements, the homography vector $\boldsymbol{h}$ was directly used to calculate the actual Y, Z positions of all tracked particles. For $X - Z$ plane measurements, the homography vectors $\boldsymbol{h}_\mathbf{F}$ and $\boldsymbol{h}_\mathbf{B}$ were estimated from calibration planes on the front (Y_F) and back (Y_B) sides of the vessel, respectively. The resulting particle positions X, Z at the measured depth Y were then calculated as a linear combination of the positions X_F, Z_F on the front side and X_B, Z_B on the back side of the vessel, where α is the normalized depth of the measurement plane Y:

$$\begin{pmatrix} X \\ Z \end{pmatrix} = (1 - \alpha) \begin{pmatrix} X_F \\ Z_F \end{pmatrix} + \alpha \begin{pmatrix} X_B \\ Z_B \end{pmatrix}, \quad \alpha = \frac{Y - Y_F}{Y_B - Y_F}. \tag{2}$$

Trajectory evaluation and filtering After the perspective correction, the coordinates of each tracked particle were extracted, and the particle trajectories were fitted with a second-order polynomial, using the least-squares method. The first derivative of the polynomial fit was used to calculate the actual velocities $\boldsymbol{u} = [u_1, u_2]$ at each particle position. To filter out invalid trajectories, several validity conditions were introduced (see Tab. 1). Condition (a) states that a given particle must be tracked in at least ten consecutive frames, ensuring a minimum tracking time of 10^{-2} s. Conditions (b) and (c) are related to the distance the particle travels. The distance is limited from below by the camera resolution (the tracked particle must travel at least a distance equal to the size of 2 px, which filters out subpixel particle motion) and from above by the tip speed of the stirrer $|u_{\mathrm{tip}}|$, which is expected as the maximum velocity in the vast majority of the vessel and for which the respective maximal possible traveled distance between consecutive frames is calculated. The last condition (d) is related to the quality of the trajectory polynomial fit, whose variance from the positions of the tracked particles must not be greater than the measurement uncertainty, i.e., half the pixel width L_{px} squared.

Table 1: Summary of validity conditions for evaluated particle trajectories.

	Description of parameter	Validity condition
a)	The minimum number of images in which a particle is detected.	10
b)	The minimum distance traveled by a particle.	1.2 mm (2 px)
c)	The maximum distance a particle can travel between two frames, based on the tip speed of the stirrer.	$\lvert u_{\mathrm{tip}}\rvert / f$
d)	The maximum variance of the predicted particle positions compared to the measured ones.	$\left(L_{\mathrm{px}}/2\right)^2$

Mean velocity and turbulent kinetic energy fields calculations The individual velocity components $u_{1,j}$ and $u_{2,j}$, evaluated in each point of all valid trajectories, were sorted into corresponding bins of size 10×10 mm. In each bin, the corresponding mean (spatial and temporal) velocity components $\overline{u}_1$, $\overline{u}_2$,

$$\overline{u}_i = \frac{\sum_{j=1}^{N} u_{i,j}}{N}, \; i = 1, 2, \tag{3}$$

and the resultant mean velocity $\overline{u}_{12}$, as well as the turbulent kinetic energy k, were evaluated. The computation of k was performed under the assumption of isotropic turbulence:

$$k = \frac{1}{2}\left(\overline{u_1'^2} + \overline{u_2'^2} + \overline{u_3'^2}\right) \approx \frac{3}{4}\left(\overline{u_1'^2} + \overline{u_2'^2}\right), \quad \overline{u_i'^2} = \frac{\sum_{j=1}^{N}\left(u_{i,j} - \overline{u}_i\right)^2}{N}, \; i = 1, 2, \tag{4}$$

where the prime symbol over u_i denotes instantaneous velocity fluctuations (sample velocity variance).

4 PTV performance metrics and results

Flow-following behavior of seeding particles One essential property of systems measured with the PTV technique is the ability of seeding particles to follow flow trajectories. This ability can be quantified by the dimensionless Stokes number,

$$St = \frac{\tau_{\mathrm{P}}}{\tau_{\mathrm{F}}} = \frac{\rho_{\mathrm{P}}\overline{d_{\mathrm{P}}}^2}{18\mu}\frac{|\boldsymbol{u}|}{L}, \tag{5}$$

which is defined as the ratio of the particle characteristic time to the flow characteristic time, and where ρ_{P} is the particle density, $\overline{d_{\mathrm{P}}} = 250\,\mu\mathrm{m}$ is the mean particle diameter, μ is the fluid viscosity, $|\boldsymbol{u}|$ is the velocity magnitude, and L is the characteristic dimension of the flow. Generally, the recommended value of St should not exceed 0.1, which ensures a velocity difference between the particle and the flow of ≈ 1% [4].

To illustrate the flow-following behavior, the worst-case scenario was chosen, which is the configuration with 1-PBT at the rotational speed of $3.75\,\mathrm{s}^{-1}$, when the highest flow velocities are achieved. Fig. 2 a) shows the distribution of the critical characteristic flow dimension $L(St = 0.1)$, calculated from Eq. (5) with constant $St = 0.1$, indicating the minimal L that can be accurately tracked using PTV at a given flow velocity. The color scale is chosen from 200 µm (the smallest possible characteristic dimension given by the particle size) to 20 mm, which is twice the edge length of the bin in which the resulting velocity obtained from the PTV is averaged (i.e., it is the resolution given by the PTV data evaluation methodology). The figure shows that approximately 98% of the cross-sectional area (≈ 0.3% of the vessel volume) has L below the PTV's resolution limit. Only in the area of the stirrer discharge, where the velocity magnitudes exceed approximately 0.3 m/s, is the critical characteristic dimension $L > 20$ mm. This indicates that the averaged velocity field obtained from the PTV is distorted in this area by means of the particle inertia, providing only limited insight into this particular zone of the flow field.

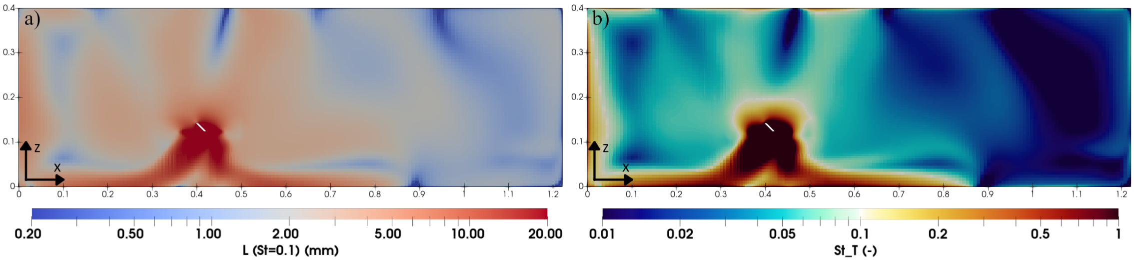

Figure 2: (a) Distribution of the critical (minimum) characteristic flow dimension L for $St = 0.1$ in the worst-case configuration (1-PBT, $N = 3.75\,\mathrm{s}^{-1}$, plane 5 cm in front of the impeller). (b) Distribution of the Stokes number St_T The averaged velocity field for estimation of $L(St = 0.1)$ was obtained from [2].

To assess the suitability of PTV measurements for estimating the turbulent kinetic energy k distribution, the Taylor microscale [5], estimated with the presumption of isotropic turbulence as

$$L_\mathrm{T} \approx \sqrt{10\frac{\nu k}{\epsilon}}, \tag{6}$$

was used as the characteristic dimension of the flow, which encompasses the vast majority of energy-containing turbulent structures. The distribution of the Stokes number St_T using L_T as the characteristic dimension is shown in Fig. 2 b). It can be seen that, similarly to Fig. 2 a), the zone of $St_\mathrm{T} > 0.1$ is situated mainly in the impeller discharge region, occupying approximately 13% of the area and 17.5% of the vessel volume, respectively. This means that some velocity fluctuations cannot be tracked appropriately, and the k estimate in the discharge region may be underestimated. To obtain the averaged velocity $\overline{u}$, turbulent kinetic energy k, and mean dissipation rate ϵ fields for the L and St calculations, the CFD simulation (RANS, $k-\epsilon$ turbulence model, multiple reference frame approach) described in detail in our parallel contribution [2] was used.

Table 2: (a) Summary of the studied stirrer configurations and (b) metrics of tracked and valid instantaneous velocities.

a)			b)		
Stirrers config.	$\overline{G}$ (s^{-1})	N (s^{-1})	n_total ($\times 10^8$)	n_valid ($\times 10^8$)	**Recovery ratio**
1-RT	40	1.25	0.480	0.355	0.74
	100	2.20	2.76	2.10	0.76
2-RT	40	1.00	1.43	1.00	0.70
	100	1.80	1.38	1.04	0.75
1-PBT	40	2.00	2.50	1.74	0.70
	100	3.75	2.29	1.64	0.71
2-PBT	40	1.60	2.15	1.57	0.73
	100	2.95	2.59	1.90	0.73

Number of tracked particles The total number of particles tracked using the TracTrac software, n_total, and the number of valid particles, n_valid (according to the conditions in Tab. 1), vary depending on the specific configuration and measurement plane. For the front plane 5 cm in front of the stirrer, the numbers are on the order of 10^8. For measurements with PBT, n_total and n_valid are relatively consistent across all four configurations, whereas there are significant differences in the RT configurations. These differences are mainly due to the direction of liquid pumping by the stirrers (axial/radial), their number (single-/double-configuration), and the relative density of particles that tend to settle. All PBT configurations generate, compared to RT at the same mean velocity gradient $\overline{G}$, a strong downward flow that tends to carry particles from the bottom back into the vessel volume. In contrast, the RT configurations have about 40% lower stirrer speeds at the same $\overline{G}$ and pump radially. For this reason, there is a gradual settling of particles in parts with low velocity (typically the corners of the vessel away from the stirrer) and a loss of suspended particles in the vessel volume, which is manifested mainly in 1-RT configuration at $N = 1.25\,\mathrm{s}^{-1}$. The average recovery ratio, despite the discrepancies in the total number of tracked particles, is (73 ± 2) % for all measurements in this plane ($n_{\mathrm{valid}}/n_{\mathrm{total}}$). Data for all configurations are summarized in the Tab. 2 b). For the studied 1-RT

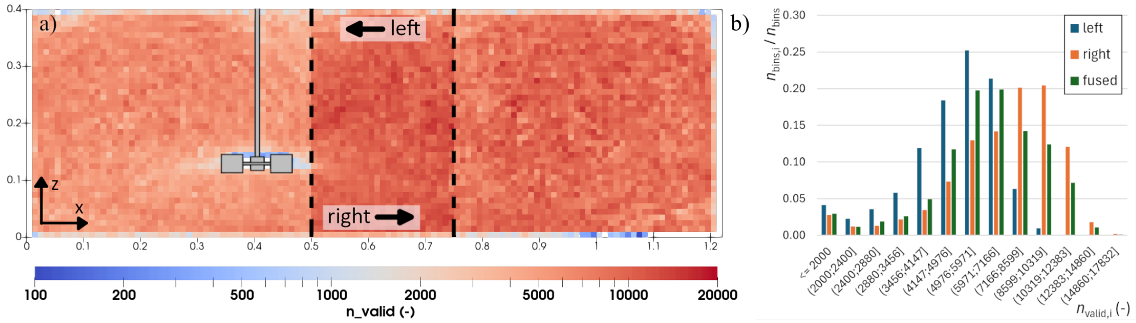

Figure 3: (a) Distribution of number of valid tracked particles n_{valid} (velocities) in configuration 1-RT, $N = 1.25\,\mathrm{s}^{-1}$. Black lines divide the fused front plane to the left and right measured parts. In the overlapping section, the n_{valid} is the sum from both sides. (b) Histogram of n_{valid} in the left, right, and fused measurement planes.

configuration at a rotational speed of $N = 1.25\,\mathrm{s}^{-1}$, the spatial statistics confirm that the mixing performance remains robust despite the gradual settling process (see Fig. 3). The cross-sectional distribution in 5 cm in front of the impeller and the corresponding histogram indicate that particle depletion occurs uniformly rather than being localized, suggesting the absence of pronounced dead zones or preferential accumulation regions. This implies that the underlying flow structures remain effective at redistributing particles throughout the vessel, and that settling primarily reduces the overall particle count without significantly compromising spatial homogeneity.

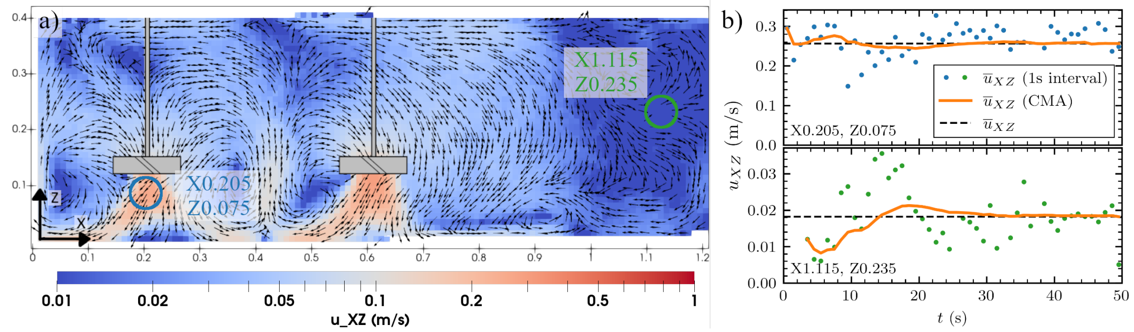

Figure 4: (a) Average velocity field measured for the 2-PBT configuration, $N = 1.6\,\mathrm{s}^{-1}$ with the marked averaging bins in the fast (blue) and slow (green) flow regions. (b) Evolution of the instantaneous velocity magnitude (1 s average) and the cumulative moving average of the velocity magnitude in the fast and slow flow regions.

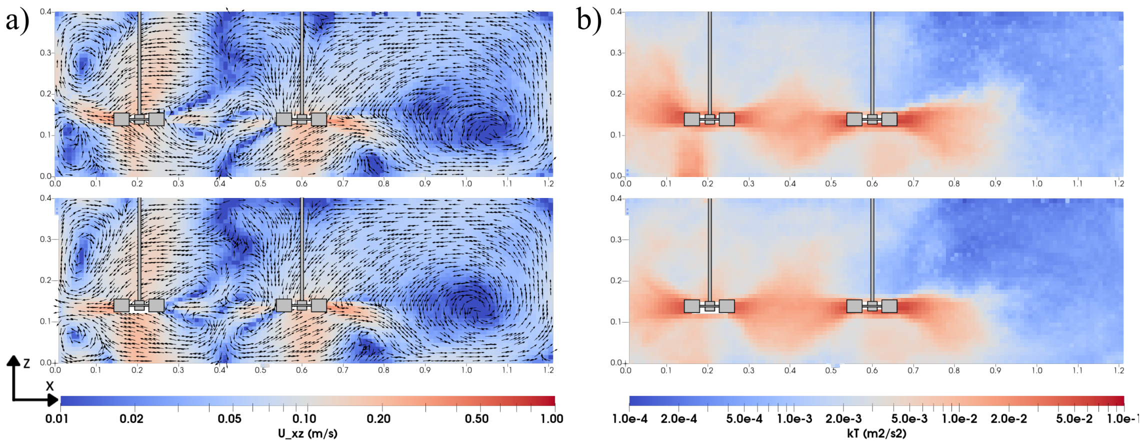

Figure 5: Distribution of (a) average velocity and (b) turbulent kinetic energy in two independent measurements in the 2-RT configuration, $N = 1.80\,\mathrm{s}^{-1}$.

Image acquisition duration Based on the measured velocity fields, it was verified that the 50 s recording time is sufficient to capture even low-frequency velocity fluctuations in parts of the vessel at larger distance

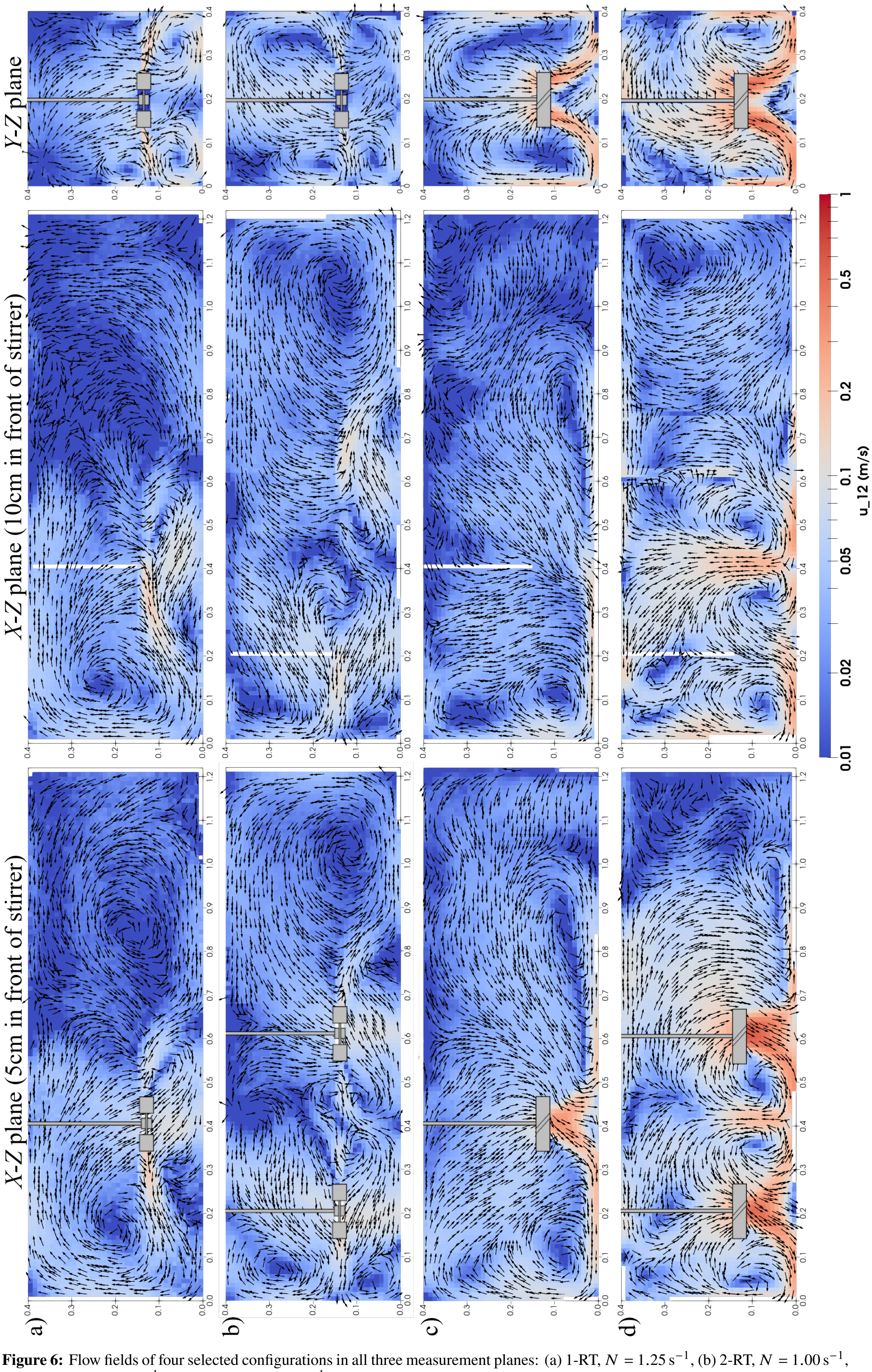

Figure 6: Flow fields of four selected configurations in all three measurement planes: (a) 1-RT, $N = 1.25\,\mathrm{s}^{-1}$, (b) 2-RT, $N = 1.00\,\mathrm{s}^{-1}$, (c) 1-PBT, $N = 2.00\,\mathrm{s}^{-1}$, (d) 2-PBT, $N = 2.95\,\mathrm{s}^{-1}$.

from the impeller, with a slow flow. The configuration with 2-PBTs and a rotation speed of $1.6\,\mathrm{s}^{-1}$ was chosen as a demonstration case. Fig. 4 a) shows the averaged velocity field from the front view, 5 cm in front of the stirrers, with two marked bins in the zone of fast (blue circle, $|\overline{u}_{XZ}| = 0.28\,\mathrm{m/s}$) and slow (green circle, $|\overline{u}_{XZ}| = 0.018\,\mathrm{m/s}$) flow. For these two bins, the instantaneous velocity magnitudes (averaged velocities over a time interval of 1 s), their cumulative moving average (CMA), and the resulting average velocity magnitude are shown in Fig. 4 b). The figure shows that while in the case of fast flow, the cumulative moving average stabilizes at the final average velocity almost immediately, in the case of 10× slower flow in the right part of the vessel, it takes about 30 s for the average velocity to stabilize at the final value $\overline{u}_{XZ}$.

Repeatability of the measurements To verify the repeatability of the measurements, selected configurations of stirrers and measuring planes were measured multiple times. Fig. 5 shows the averaged velocity field $\overline{u}_{XZ}$ and the distribution of turbulent kinetic energy k in the 2-RT vessel configuration at a speed of $1.80\,\mathrm{s}^{-1}$. Both data sets are in good agreement for both monitored quantities. A qualitative discrepancy is observed in the left part of the vessel: in the first measurement (top row), the main flow leaving the left impeller is slightly twisted upwards compared to the second one, which is also visible in the k distribution. In general, the repeatability of the measurements is satisfactory with regard to the use of PTV for validating RANS simulations in pilot-scale stirred vessels.

Results The resulting flow fields of the four selected configurations and all three measurement planes are shown in Fig. 6.

5 Conclusions

The contribution presents a method for obtaining experimental validation data for CFD simulations of flow in pilot-scale stirred vessels using particle tracking velocimetry (PTV). A large-scale PTV measurement and evaluation methodology for velocity fields measurements was developed and tested on an experimental arrangement of a rectangular stirred vessel with variable stirrer configuration and rotation speed. It is shown that for the validation of RANS simulations, the methodology provides a good compromise between the reliability of the measured fields and the feasibility of measurements in pilot-scale vessels, especially in terms of the physical limitations of other available experimental techniques and the time and financial demands. The paper discusses shortcomings that mainly concern distorted velocity fields in fast flow at the stirrer outlet, inaccuracies in estimating the distribution of turbulent kinetic energy, or particle sedimentation in slow flow in a configuration with a Rushton turbine. The fields obtained by the PTV presented in this work were successfully used for the CFD simulations validation in the parallel contribution [2].

Acknowledgment

The work on this paper was supported by the institutional support *RVO:67985874*. The research was funded by the *Czech Science Foundation (GAČR)* under the *Grant No. 25-17383S*. The participation of OG and VB was financially supported by the *grant of Specific University Research A1_FCHI_2025_004*. Computational resources were provided by the *e-INFRA CZ project (ID:90254)*, supported by the *Ministry of Education, Youth and Sports of the Czech Republic*.

References

[1] R. L. McKenzie, "Measurement capabilities of planar doppler velocimetry using pulsed lasers," *Appl. Opt.*, vol. 35, pp. 948–964, Feb 1996.

[2] V. Bílek, O. Gebouský, and J. Haidl, "CFD simulation methodology validated for mixed rectangular tank equipped with single and multiple impellers," in *Topical Problems of Fluid Mechanics*, (Prague, Czech Republic), 2026. (accepted contribution).

[3] J. Heyman, "Tractrac: A fast multi-object tracking algorithm for motion estimation," *Computers & Geosciences*, vol. 128, pp. 11–18, 2019.

[4] M. Raffel, C. J. Willert, F. Scarano, C. J. Kähler, S. T. Wereley, and J. Kompenhans, "Particle Image Velocimetry: A Practical Guide," 2018.

[5] T. Watanabe, X. Zhang, and K. Nagata, "Turbulent/non-turbulent interfaces detected in DNS of incompressible turbulent boundary layers," *Physics of Fluids*, vol. 30, p. 035102, 03 2018.